Contrib Mineral Petrol (2003) 146: 62–77
DOI 10.1007/s00410-003-0482-x

ORIGINAL PAPER

James A. Walker · Kurt Roggensack · Lina C. Patino
Barry I. Cameron · Otoniel Matías

The water and trace element contents of melt inclusions across an active subduction zone

Received: 1 October 2002 / Accepted: 23 April 2003 / Published online: 28 June 2003

Abstract Water concentrations of olivine-hosted melt inclusions show no consistent variation across the northern part of the Central American subduction zone in southeastern Guatemala. Magmatic water contents remain moderately high (~2 wt%) throughout the back-arc region. Melt inclusions from some of these back-arc basalts also have notably high CO_2 contents (> 900 ppm CO_2). The B and B/Ce ratios of melt inclusions systematically decline across the arc, the first parameters to exhibit systematic changes across southeastern Guatemala. It appears, therefore, that dehydration-driven, flux-melting persists across the arc, although decompression melting is of approximately equal importance in the back-arc region. Dehydration of the slab/wedge region is regarded as semi-continuous down-dip, to depths of at least 175–200 km. Moderate water contents are maintained by stepwise dehydration reactions, while truly incompatible fluid mobile elements are progressively stripped from the Cocos plate. The notably high CO_2 contents of some back-arc basalts may indicate increasing devolatilization of subducted carbonate sediments with slab depth. The moderate H_2O contents of back-arc basaltic magmas has likely contributed to their early fractionation of clinopyroxene around the Moho.

J. A. Walker (✉)
Department of Geology and Environmental Geosciences,
Northern Illinois University, DeKalb, IL 60115, USA
E-mail: jim@geol.niu.edu
Tel.: +1-815-7537936
Fax: +1-815-7531945

K. Roggensack
Department of Geological Sciences,
Arizona State University, Tempe, AZ 85287-1404, USA

L. C. Patino
Department of Geological Sciences,
Michigan State University, East Lansing, MI 48824-1115, USA

B. I. Cameron
Department of Geosciences,
University of Wisconsin-Milwaukee,
Milwaukee, WI 53201, USA

O. Matías
Seccion Vulcanología, INSIVUMEH, 7a Ave 14-57,
Zona 13, Guatemala City, Guatemala

Editorial responsibility: T.L. Grove

Introduction

Water plays a critical role in the generation and evolution of subduction zone magmas (e.g., Yoder 1969; Ringwood 1974). For instance, hydrous fluid released from subducted lithosphere is likely the principal catalyst for partial melting of the overlying mantle wedge and the production of primary basaltic magmas at subduction zones (McBirney 1969; Ringwood 1974; Sakuyama and Nesbitt 1986; Tatsumi 1986; Bizimis et al. 2000). Moreover, the amount of H_2O influences the major element compositions of the resultant basaltic magmas (Kushiro 1969, 1972; Green 1973; Mysen and Boettcher 1975; Hirose and Kawamoto 1995; Gaetani and Grove 1998; Ulmer 2001). And lastly, the relative stabilities of minerals that subsequently crystallize from wedge-generated magmas is critically dependent on their overall H_2O concentrations (Osborn 1959; Cawthorn and O'Hara 1976; Boettcher 1977; Carr et al. 1981; Grove and Baker 1984; Baker and Eggler 1987; Sisson and Grove 1993; Gaetani et al. 1993; Müntener et al. 2001; Danyushevsky 2001).

Subduction zone basaltic magmas are distinguished by H_2O contents that exceed those of mid-ocean ridge (MORB) and ocean-island (OIB) basalts (Anderson 1974; Garcia et al. 1979; Harris and Anderson 1984; Hochstaedter et al. 1990; Sisson and Layne 1993; Sobolev and Chaussidon 1996; Roggensack et al. 1996, 1997; Newman et al. 2000; Roggensack 2001a, b), although there are noteworthy exceptions (Sisson and Bronto 1998). Moreover, analyses of melt inclusions indicate that some subduction zone basaltic magmas have strikingly high pre-eruptive H_2O concentrations, in excess of 3 wt% (Harris and Anderson 1984; Sisson and

Layne 1993; Roggensack et al. 1996, 1997; Newman et al. 2000; Roggensack 2001; Luhr 2001). Presumably such elevated H_2O contents are an inheritance from hydrous magma generation (Sisson and Layne 1993; Stolper and Newman 1994; Newman et al. 2000).

Geochemical studies across subduction zones have yielded important insights into the transfer of hydrous fluids from subducted lithosphere to mantle wedge and subsequent magma generation (Ishikawa and Nakamura 1994; Ryan et al. 1995, 1996; Hoogewerff et al. 1997; Ishikawa and Tera 1997; Woodhead et al. 1998; Walker et al. 2000; Churikova et al. 2001). Using mineralogical inferences, a number of studies have suggested that magmatic H_2O contents increase across subduction zones (Sakuyama 1979; Gill 1981; Morrice and Gill 1986; Tatsumi et al. 1991). Quantitative analyses of melt inclusions, however, indicate that behind-the-front or back-arc magmas have equivalent or lower, not higher, H_2O concentrations than magmas erupted at the volcanic front (Garcia et al. 1979; Hochstaedter et al. 1990; Newman et al. 2000). Here we use olivine-hosted melt inclusions to systematically examine how magmatic H_2O concentrations, and other element contents, vary across an active subduction zone, the Central American subduction zone, and the implications those variations have for magma generation and differentiation.

Geologic setting

The Central American subduction zone extends over 1,200 km from Guatemala to central Costa Rica (Fig. 1). It is one of the most active subduction zones with estimated extrusion rates an order of magnitude higher than those of most other subduction zones (90–100 $km^3 my^{-1} arc\ km^{-1}$ versus 4–9 $km^3 my^{-1} arc\ km^{-1}$; Patino et al. 2000; Sigurdsson 2000). The subduction zone becomes tectonically more complex in Guatemala due to the presence of the North American/Caribbean transform boundary (Fig. 1). Left-lateral motion along this boundary has led to singular arc-normal intra-arc and back-arc extension (Fig. 1; Burkart and Self 1985). Extension has been accompanied by abundant volcanism behind the volcanic front in southeastern Guatemala and western El Salvador, allowing a near-continuous examination of geochemical variations across some 125 km of the subduction zone (Fig. 1). The active volcanic front in this region is composed of several large polygenetic composite volcanoes, such as Pacaya and Tecuamburro (Fig. 1), built via eruptions of a wide variety of magmas, including basaltic magmas. Recent volcanism behind the volcanic front, in contrast, largely consists of numerous small monogenetic cinder cones built exclusively from basaltic magmas (Walker 1981).

Sampling and analytical methods

In 1999, basaltic lapilli from scoria/ash falls were collected on the flanks of Pacaya Volcano on the Guatemalan volcanic front and from four quarried cinder cones at systematically greater distances behind the front in southeastern Guatemala. Basaltic pyroclastics were

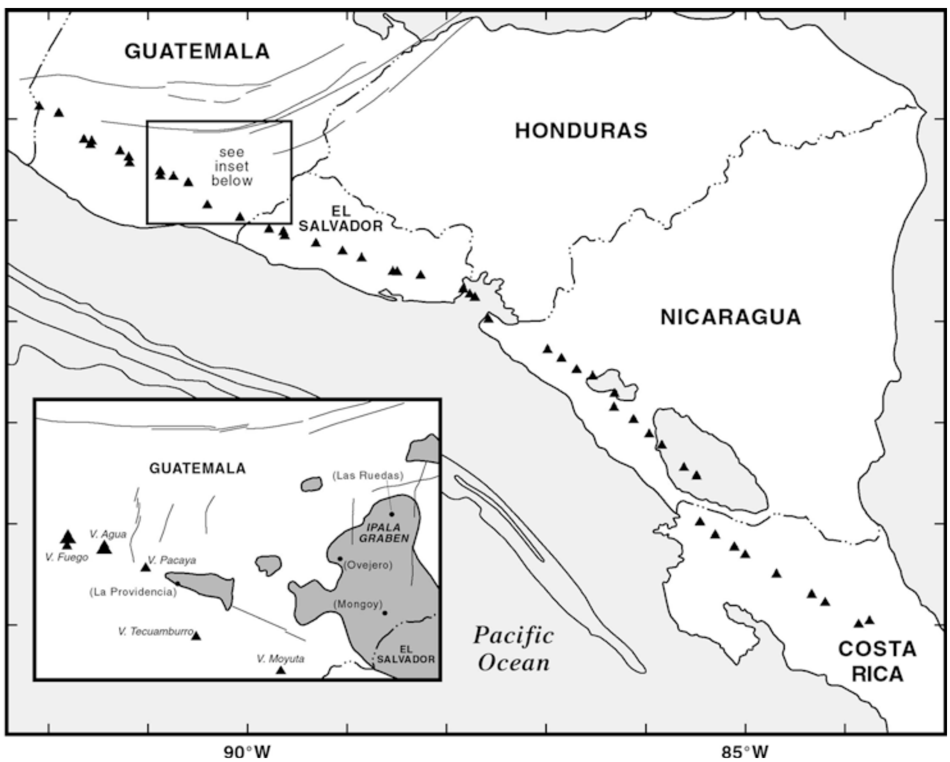

Fig. 1 Volcanic front of the Central American subduction zone. *Solid lines* through central Guatemala are faults associated with the North American/Caribbean transform boundary. *Inset* bounds study area. *Solid lines* are faults; *shaded areas* approximately outline areas of recent behind-the-front or back-arc monogenetic volcanism. *Small dots* show cinder cones sampled behind the volcanic front

targeted rather than basaltic lavas because their rapid quenching reduces the amount of post-entrapment modification in melt inclusions (Clocchiatti 1975; Roedder 1984). Also, melt inclusions from basaltic lavas are often crystalline and unsuitable for volatile analysis (Cervantes and Wallace 2003). At Pacaya, a sample was taken from the scoria fall deposited during the November 1996 eruption. Cinder cones sampled behind the front include La Providencia, Cerro Las Ruedas, Cerro Mongoy and Cerro Ovejero. Approximate locations of these cones are shown in Fig. 1.

Individual olivine crystals were handpicked from all of the sampled tephras and examined with a binocular microscope to locate unfractured melt inclusions. Crystals with suitable melt inclusions were then prepared for major, volatile and trace element analyses as described by Roggensack (2001a, 2001b). Analyzed melt inclusions were round or ovoid with negative crystal shapes. All melt inclusions were brown in color and contained a single vapor bubble. The sizes of analyzed melt inclusions was predominantly between 45 and 85 microns, although some from Cerro Las Ruedas were as large as 125 μm. The major element, S and Cl contents of melt inclusions were determined by electron microprobe microanalysis at Arizona State University. Water and CO_2 concentrations of melt inclusions were ascertained by Fourier transform infrared spectroscopy (FTIR) at the laboratory of J. Lowenstern of the USGS in Menlo Park, California. Trace element analyses of melt inclusions were done via secondary ion mass spectrometry (SIMS) at Arizona State University or laser ablation inductively coupled plasma mass spectrometry (LA-ICPMS) at Michigan State University. Analytical particulars for the microprobe, ion probe and the FTIR analyses can be found in Roggensack (2001a, 2001b). At Michigan State, concentrations for Ba and La in melt inclusions were determined with a Cetac LSX-200+ and Micromass Platform ICP-MS. The Cetac LSX-200+ is an Nd:YAG laser with a frequency quadrupled to an UV wavelength of 266 nm. Laser ablation parameters used included a spot size of 25 μm and frequency of 20 Hz. The ablation mode was depth profile, where the sample stage was raised at a rate of 1 μm/s. The data acquisition started before the ablation. After ~0.3 min of data acquisition, ablation was initiated and continued for 15 s. The first 0.3 min of data acquisition were used to measure the background. Once the ablated material reached the detector, the signal for the different elements was clearly observed in well-developed peaks. The results were quantified using the height of the peak above background for each element. The concentrations were calculated following Norman et al. (1996), with NIST 612 glass as the external standard and calcium as the internal standard. The accuracy of the method was tested by analyzing BHVO−1(as a fused lithium metaborate glass disk) as an unknown. The determined values of La and Ba were 17.11 and 129.44 ppm, respectively, within 10% of their reference values.

In addition to our new data for Pacaya, previously published melt inclusion data from the 1974 eruption of Fuego Volcano (Fig. 1) were used to characterize water contents along the volcanic front (or VF) (Harris and Anderson 1984; Sisson and Layne 1993; Roggensack 2001b). New volatile data are given in Table 1. Trace element concentrations of melt inclusions are presented in Table 2.

Despite their rapid quenching, melt inclusions from basaltic pyroclasts are still vulnerable to post-entrapment crystallization which could alter their primary compositions (Bureau et al. 1998a, b; Luhr 2001). Where possible, we have checked our melt inclusions for post-entrapment crystallization by examining their Fe-Mg partitioning with their host olivines. If the observed K_D $[(FeO/MgO)_{olivine}/(0.89FeO^T/MgO)_{melt\ inclusion}]$ is below our assumed equilibrium value of 0.312 (Ulmer 1989), then we have iteratively added 1 wt% of the host olivine composition to the melt inclusion composition until the equilibrium value is approached (Sobolev and Shimizu 1993; Sisson and Layne 1993; Kamenetsky et al. 1995; Lee and Stern 1998; Bureau et al. 1998a, b; Marianelli et al. 1999; Luhr 2001). Calculated amounts of added olivine are significant, ranging from 0–7 wt%, with an average of 2–3 wt%. Therefore, in all diagrams and

Table 1 New melt inclusion volatile concentrations

Sample	Volcano	BVF distance (km)[a]	H_2O (wt%)[b]	CO_2 (ppm)[c]	SO_3 (wt%)	Cl (wt%)
gpa5–11	Pacaya	–	2.4	–	–	0.10
gpa5–13	Pacaya	–	2.0	–	0.10	0.10
gpa5–15a	Pacaya	–	2.0	–	–	0.12
gpa5–18a	Pacaya	–	1.7	–	0.23	0.11
gpa5–19a	Pacaya	–	1.7	–	–	0.09
gpa5–20	Pacaya	–	1.7	–	0.26	0.11
gpa5–28	Pacaya	–	1.7	–	0.42	0.12
gu25–1a	BVF1[d]	15.7	0.53	–	0.09	0.07
gu25–3	BVF1	15.7	0.80	–	0.11	0.07
gu25–4	BVF1	15.7	0.30	352	0.02	0.06
gu25–7	BVF1	15.7	1.02	–	0.16	0.08
gu25–9	BVF1	15.7	1.02	–	0.26	0.03
gu37–1	BVF2[e]	36.4	2.11	999	–	–
gu37–2	BVF2	36.4	1.78	812	0.22	0.07
gu37–8	BVF2	36.4	1.58	–	0.28	0.11
gu41–2	BVF3[f]	50.7	1.72	966	0.37	0.06
gu41–6	BVF3	50.7	2.06	726	0.42	0.06
gu41–8	BVF3	50.7	2.48	1062	0.34	0.07
gu41–9	BVF3	50.7	2.13	280	–	–
gu28–1	BVF4[g]	77.8	2.09	1643	0.28	0.03
gu28–2	BVF4	77.8	2.00	1306	0.24	0.04
gu28–3	BVF4	77.8	1.95	1344	0.27	0.01
gu28–5	BVF4	77.8	2.16	1572	0.08	0.03
gu28–8	BVF4	77.8	1.99	1292	0.32	0.04
gu28–9	BVF4	77.8	1.88	1954	0.41	0.05
gu28–10a	BVF4	77.8	2.00	2342	0.27	0.05
gu28–11a	BVF4	77.8	1.71	1280	0.24	0.01
gu28–13	BVF4	77.8	1.98	1271	0.24	–

[a]Distance behind the volcanic front measured orthogonal to the front
[b]3,500 cm^{-1} FTIR data
[c]Average of 1,410 and 1,510 cm^{-1} FTIR data
[d]La Providencia cinder cone
[e]Cerro Mongoy
[f]Cerro Ovejero
[g]Cerro Las Ruedas

discussions that follow involving the major constituents of the melt inclusions, i.e., SiO_2, Al_2O_3, FeO, MgO and CaO, only recalculated compositions are utilized. One inherent flaw to this recalculation method, however, is that it neglects any episodes of relatively slow cooling experienced by the olivine crystal, prior to explosive eruption, during which diffusive re-equilibration between crystal and melt inclusion may have occurred (Danyushevsky et al. 2000; Gaetani and Watson 2000). Olivine-corrected major element compositions of selected melt inclusions are provided in Table 3. Complete microprobe analyses are available from the second author on request.

Results

Previous melt inclusion studies have shown that basic magma erupted from Fuego Volcano in 1974 had highly variable pre-eruptive H_2O contents, ranging from 1–6.2 wt% (Harris and Anderson 1984; Sisson and Layne 1993; Roggensack 2001b; Fig. 2a). According to Roggensack (2001b), the observed variability is a reflection of magma hybridization immediately before the eruption and that pre-mixing water contents of basaltic magma were likely 4–5 wt%. Similarly, elevated water contents have also been measured in basaltic melt inclusions from Cerro Negro Volcano in Nicaragua (Roggensack et al. 1997) and Parícutin Volcano in Mexico (Luhr 2001), and have been generally inferred for some subduction zone basalts (Sisson and Grove 1993; Grove et al. 2002). The water concentrations of melt inclusions from the 1996 eruption of Pacaya Volcano, by contrast, are less variable and lower than at Fuego, hovering around 2 wt% (Fig. 2a). Pacaya's water concentrations, nevertheless, are still within the normal range for subduction zone VF basaltic magmas (Fig. 3a).

In general, water contents in behind-the-front (or BVF) basalts are similar to those at Pacaya (Figs. 2a and 3a). The one exception are the relatively low water concentrations (0.3–1.02 wt%) found in melt inclusions from La Providencia cinder cone within 20 km of the

Table 2 Trace element concentrations of melt inclusions in ppm

Sample	Volcano	BVF distance (km)[a]	B[b]	Li	Sr	Y	Zr	Ba	La	Ce
gpa5–16a	Pacaya	–	11.3	12.2	417	26	106	418	–	28
pac98–83	Pacaya	–	–	–	–	–	–	737*	21.8	–
pac98–84	Pacaya	–	–	–	–	–	–	733*	24.9	–
pac98–85	Pacaya	–	–	–	–	–	–	705*	22.3	–
gu25–1a	BVF1[c]	15.7	9.6	7.3	442	26	155	234	–	26
gu25–5	BVF1	15.7	3.8	8.4	563	14	76	122	–	14
gu37–2	BVF2[d]	36.4	7.8	7.1	503	24	127	301	–	24
gu37–5	BVF2	36.4	8.2	7.9	472	21	121	302	–	24
gu37–101	BVF2	36.4	–	–	–	–	–	428*	16.5	–
gu41–1	BVF3[e]	50.7	5.4	9.9	574	21	102	222	–	22
gu41–4a	BVF3	50.7	6.3	10.2	561	20	120	275	–	25
gu41–8	BVF3	50.7	6.9	9.2	564	22	119	257	–	26
gu41–71	BVF3	50.7	–	–	–	–	–	359*	14.1	–
gu41–72	BVF3	50.7	–	–	–	–	–	379*	16.4	–
gu41–73	BVF3	50.7	–	–	–	–	–	419*	15.7	–
gu28–5	BVF4[f]	77.8	3.8	7.2	422	22	128	43	–	18
gu28–6	BVF4	77.8	2.5	8.2	427	26	141	43	–	21
gu28–71	BVF4	77.8	–	–	–	–	–	63*	8.0	–

[a]Distance behind the volcanic front measured orthogonal to the front
[b]B, Li, Sr, Y and most Ba concentrations by SIMS; La and Ba (marked by an *asterisk*) by LA-ICPMS
[c]La Providencia cinder cone
[d]Cerro Mongoy
[e]Cerro Ovejero
[f]Cerro Las Ruedas

Table 3 Olivine-corrected, volatile-free major element analyses of representative melt inclusions (wt%)

Sample Volcano	gpa5–3 Pacaya	gpa5–16a Pacaya	gpa5–23a Pacaya	gu25–1a BVF1[a]	gu37–2 BVF2[b]	gu41–8 BVF3[c]	gu28–9 BVF4[d]
SiO_2	53.23	52.78	55.38	50.69	50.41	52.59	51.12
TiO_2	1.14	1.49	1.27	1.59	1.28	1.21	1.21
Al_2O_3	16.60	15.70	14.10	20.08	19.85	19.70	17.49
FeO^T	13.49	12.44	13.18	7.26	7.09	10.36	5.83
MnO	0.28	0.20	0.20	0.05	0.09	0.18	0.10
MgO	5.54	5.05	4.12	4.46	5.55	7.22	7.33
CaO	8.75	8.06	6.88	10.10	10.33	11.09	12.93
Na_2O	3.87	3.94	4.46	4.48	4.11	3.50	3.48
K_2O	0.79	0.95	1.03	0.97	0.94	0.82	0.29
P_2O_5	0.26	0.36	0.43	0.33	0.35	0.33	0.23
Wt% ol[e]	0.04	0.00	0.01	0.00	0.00	0.07	0.00

[a]La Providencia cinder cone
[b]Cerro Mongoy
[c]Cerro Ovejero
[d]Cerro Las Ruedas
[e]Wt% added olivine

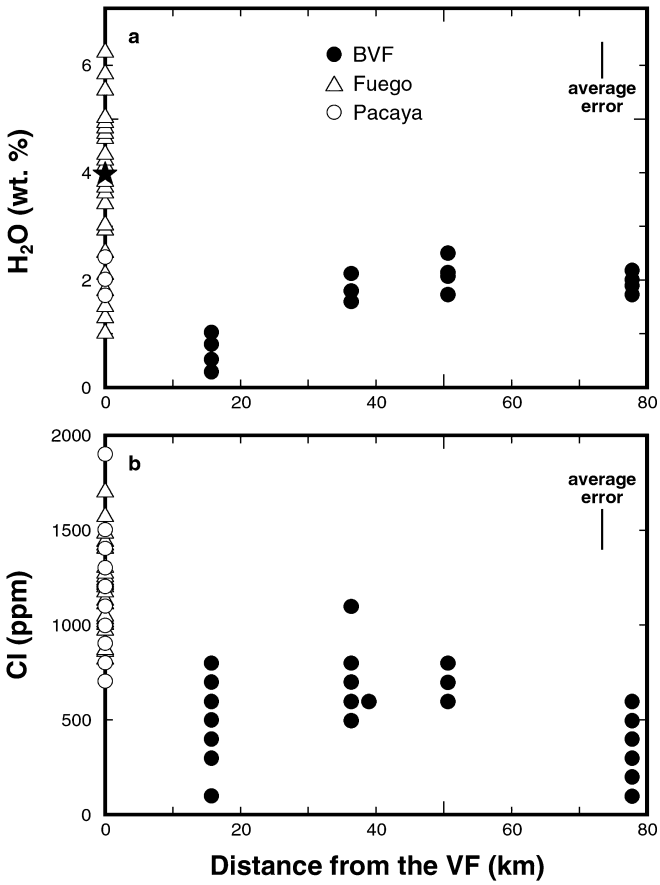

Fig. 2 Variation in H_2O (**a**) and Cl (**b**) of olivine-hosted melt inclusions across southeastern Guatemala. *Star* is average H_2O content of olivine-hosted melt inclusions from Cerro Negro Volcano in Nicaragua (Roggensack et al. 1997). The average analytical uncertainty for the measurements is shown by the *error bars* in the upper right of each diagram

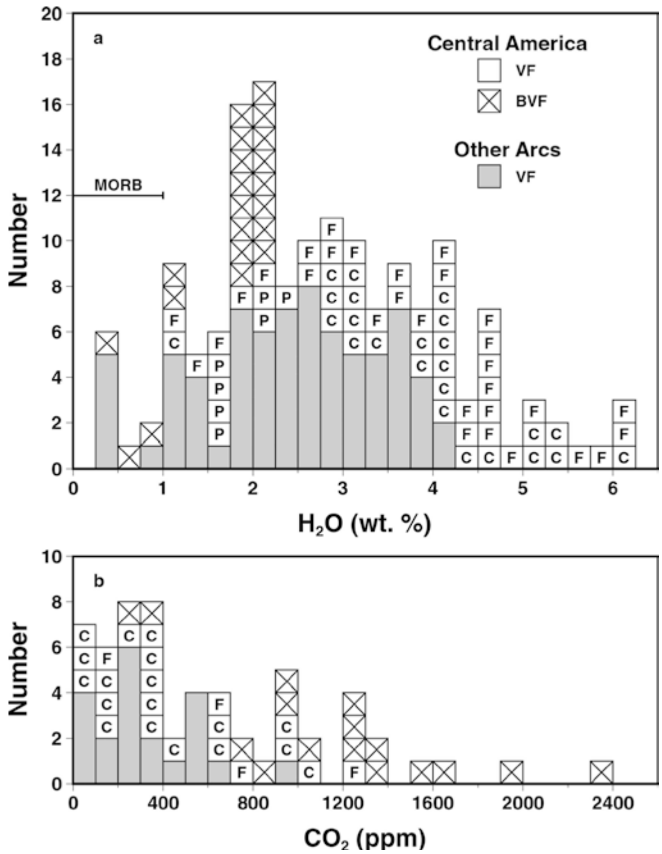

Fig. 3 Compilation of measured H_2O and CO_2 concentrations in melt inclusions from basic lavas erupted in subduction zones (*arcs*). Data from Central American volcanic front (*VF*) further subdivided by volcanic center: *F* Fuego Volcano; *C* Cerro Negro Volcano; *P* Pacaya Volcano. *BVF* are data from behind-the-front volcanoes in southeastern Guatemala. Range of H_2O concentrations in MORB from Newman et al. (2000). Sources of subduction zone data: this study; Sisson and Layne (1993); Sobolev and Chaussidon (1996); Roggensack et al. (1996); Roggensack et al. (1997); Sisson and Bronto (1998); Gioncada et al. (1998); Newman et al. (2000); Saito et al. (2001); Roggensack (2001b); Luhr (2001)

volcanic front, near Pacaya (Fig. 1). The values at this cone range between those typical of mid-ocean ridge basalts and those more characteristic of subduction zone basalts (Fig. 3a; e.g., Sobolev and Chaussidon 1996; Sisson and Bronto 1998). Overall, therefore, water concentrations show no consistent across-arc variation, although they tend to be lower and less variable behind the volcanic front (Fig. 2a). The chlorine contents of melt inclusions are also generally lower behind the front, and like water, show no regular across-arc variation (Fig. 2b). The SO_3 and CO_2 contents of VF and BVF melt inclusions show no consistent differences, ranging from <0.10–0.50 wt% and <300 – $>2,000$ ppm, respectively (Table 1; Fig. 3b).

The CO_2 concentrations of melt inclusions from the BVF cinder cones are notably high (most >500 ppm) compared to those of basaltic melt inclusions from other subduction zone volcanic rocks (Fig. 3b). The melt inclusions from Cerro Las Ruedas, the cinder cone farthest from the volcanic front (Fig. 1), are particularly CO_2-rich (Table 1). At both Fuego and the BVF volcanoes, CO_2 variation is precipitous relatively to H_2O (Fig. 4). Such trends are compatible with open-system degassing of an ascending, vapor-saturated magma (Dixon and Stolper 1995; Roggensack et al. 1997; Newman et al. 2000; Roggensack 2001a).

In many suites of terrestrial basalts, magmatic water contents correlate with incompatible element contents, most notably K (Byers et al. 1983, 1985, 1986; Aggrey et al. 1988a, b; Dixon et al. 1988; Jambon and Zimmerman 1988; Michael 1988; Muenow et al. 1990; Danyushevsky et al. 1993; Sisson and Layne 1993; Stolper and Newman 1994; Newman et al. 2000). However, no incompatible elements exhibit clear correlations with H_2O in the melt inclusions from southeastern Guatemala, except for Zr and Y, which display negative correlations for the few BVF samples analyzed for all three elements (Fig. 5a, b). Analogous negative correlations between water and incompatible element contents have been reported from melt inclusions in other arc basalts and have been attributed to concomitant crystallization and vapor exsolution on ascent (Sisson and Layne 1993). We do not think this is a viable explanation for the BVF

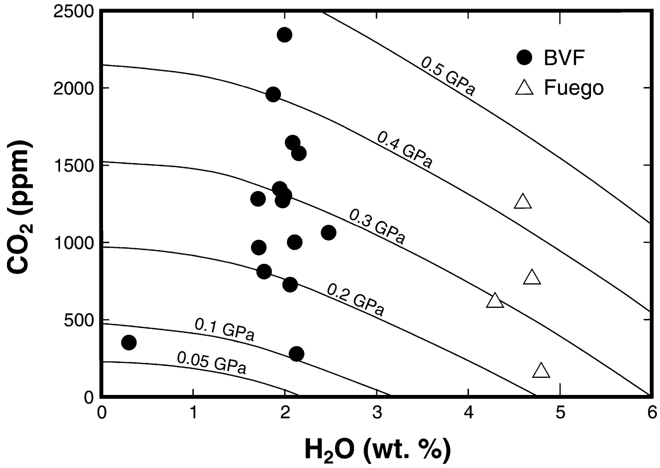

Fig. 4 CO_2 versus H_2O for BVF and Fuego melt inclusions. Vapor-saturated isobars (0.05–0.5 GPa) calculated using VolatileCalc (Newman and Lowenstern 2002)

samples because CO_2, Cl and S fail to show corresponding negative correlations with incompatible elements (e.g., Fig. 5c), and Zr and Y fail to correlate with any indices of differentiation such as Mg# (e.g., Fig. 5b). The major element concentrations of the melt inclusions from Fuego and the BVF cinder cones largely fall within the range displayed by their respective lava compositions (Fig. 6). This is much less true for Pacaya volcano (Fig. 6). Most notably, melt inclusions from Pacaya typically contain lower CaO, Al_2O_3, and higher FeO^T than Pacaya's lavas (Fig. 6).

The MgO concentrations and the Mg#'s of melt inclusions are commonly higher behind the volcanic front (Figs. 6 and 7). This suggests that, the higher chlorine, and perhaps the higher water contents, of the VF melt inclusions may be partly ascribable to their having experienced greater magmatic differentiation (Fig. 7). At equivalent MgO contents, BVF melt inclusions typically contain higher CaO, CaO/Al_2O_3, and lower FeO^T and SiO_2 than VF melt inclusions (Fig. 6). Two BVF melt inclusions from Cerro Las Ruedas, the cinder cone farthest from the volcanic front, are significantly enriched in CaO (Fig. 6a). Olivine-hosted melt inclusions with unusually high CaO contents (13 wt. %) have been found in a number of subduction zones and are believed by some to represent a distinctive magma type generated in arc environments (Della-Pasqua and Varne 1997; Schiano et al. 2000).

The Ba, Li, La, and Ce contents of melt inclusions are also, like those of water and chlorine, generally lower behind the volcanic front (e.g., Fig. 8a, b). This is likely due to the trapping of less differentiated compositions behind the volcanic front (Fig. 8c). The B concentrations of melt inclusions are also lower behind the front but more significantly, they exhibit grossly progressive declines across the arc (Fig. 9a). The B/Ce ratios of melt inclusions also systematically fall across southeastern Guatemala (Fig. 9b). Regular, declining variations were unexpected as whole-rock compositions show no

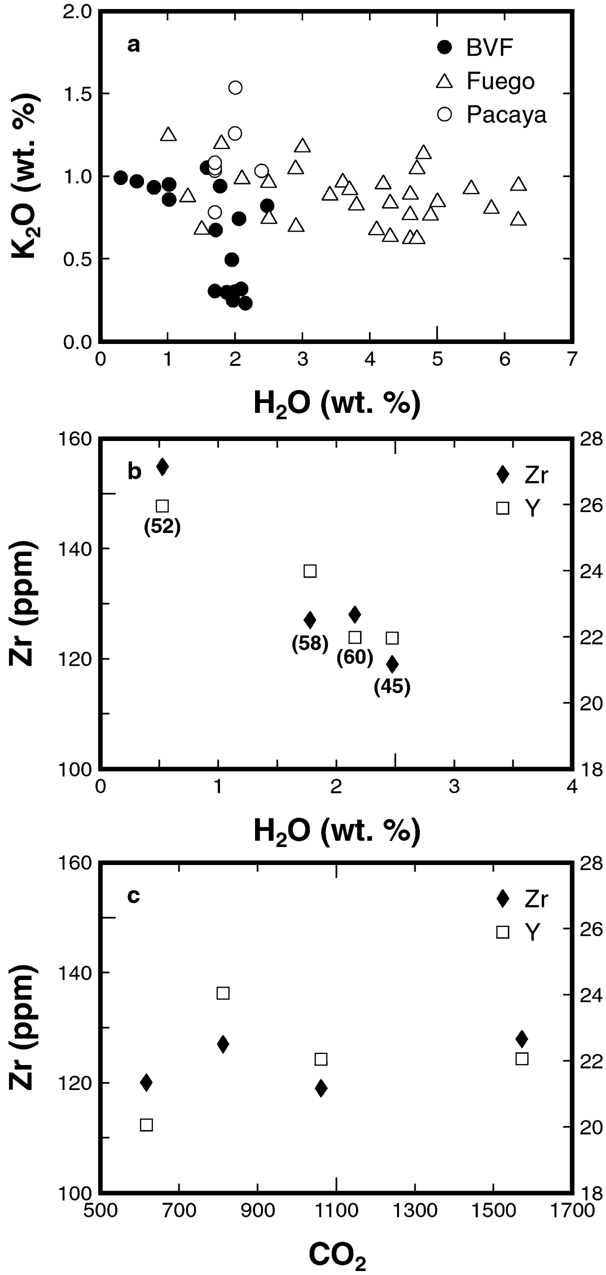

Fig. 5 **a** K_2O versus H_2O for olivine-hosted melt inclusions from southeastern Guatemala. **b** Zr and Y versus H_2O for BVF melt inclusions. *Numbers in parentheses* are Mg #'s for the four melt inclusions. **c** Zr and Y versus CO_2 for BVF melt inclusions

systematic across-arc changes in any incompatible elements or incompatible element ratios (Fig. 9; Walker et al. 1995, 2000). Other incompatible element ratios of melt inclusions, analogous to B/Ce (e.g., Ba/Zr) show no methodical across-arc variations, although BVF melt inclusions are characterized by lower values (Fig. 9c). With the exception of B, trace element contents of melt inclusions generally overlap values obtained on lava compositions (e.g., Fig. 9d). The differing B concentrations of melt inclusions and whole-rock compositions could be caused by surficial leaching of B from the lavas

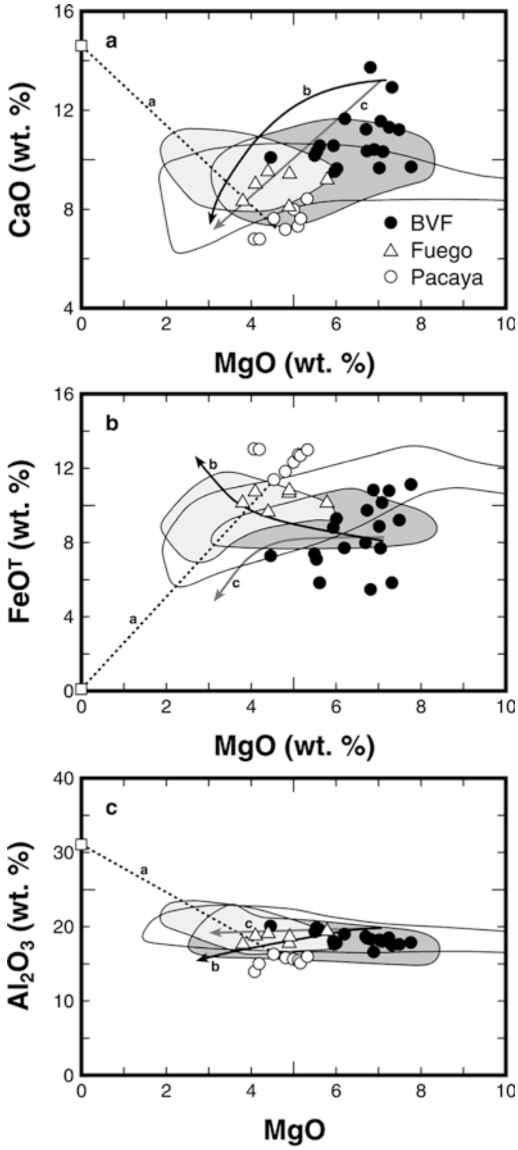

Fig. 6 CaO (**a**), FeO^T (**b**), and Al_2O_3 against MgO for melt inclusions from southeastern Guatemala. Where necessary, compositions have been recalculated for post-entrapment crystallization as described in the text. Fields outline compositional ranges of lava compositions: *darkest tone* BVF lavas; *medium tone* Pacaya lavas; *unshaded* Fuego lavas. *Open square* is a representative plagioclase (phenocryst) composition from Pacaya (Cameron 1998). *Dotted line* (**a**) illustrates compositional changes accompanying plagioclase accumulation in an average Pacaya magma. *Line b* approximates the liquid line of descent for a basalt with moderately low water contents (from experimental data on a Galapagos tholeiite from Spulber and Rutherford (1983) where $P_{H2O} = 0.7P_{Total}$). Line *c* approximates the liquid line of descent for a basalt with higher water contents (from experimental data on water-saturated Medicine Lake Highland basalts from Sisson and Grove (1993) where P = 2 kb)

or B loss during eruptive degassing (Higgins 1988; Schmidt et al. 2002). The likelihood of B mobility at the surface has been bolstered by Patino et al. (1998, 2002) and Cameron (1998) who have demonstrated that the trace element compositions of some Late Tertiary to early Quaternary lavas from southeastern Guatemala,

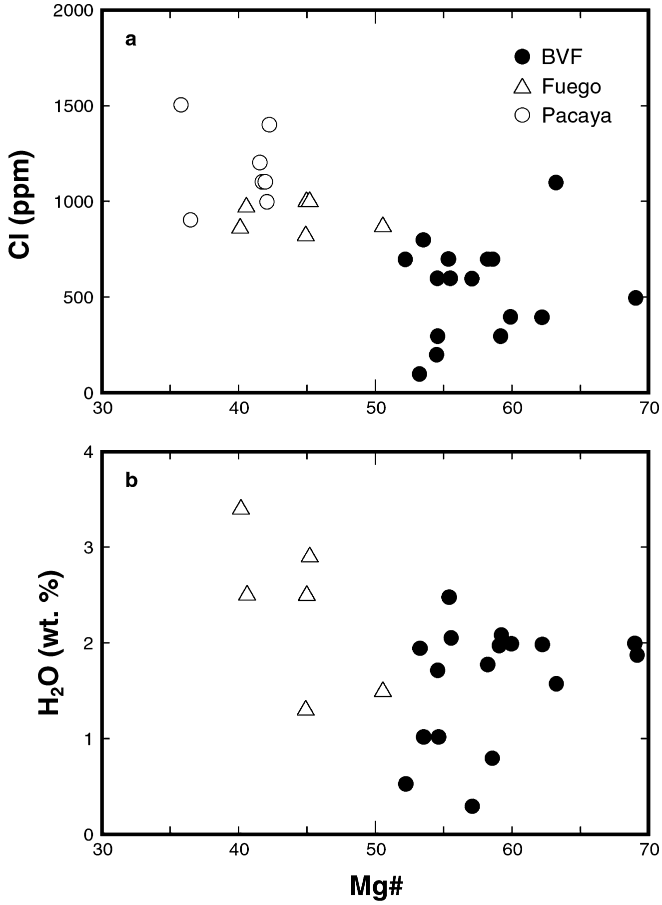

Fig. 7 Cl (**a**) and H_2O (**b**) versus Mg# (100 Mg/[Mg + Fe^{2+}]) for melt inclusions from southeastern Guatemala

lavas that lack megascopic or major element evidence of alteration, can be significantly affected by incipient weathering. Therefore, we think the systematic across-arc variations in B and B/Ce are real and suggest that the trace element contents of the olivine-hosted melt inclusions, being shielded from surface weathering, are more reliable than whole-rock values for evaluating petrogenesis across subduction zones. Moreover, it has been convincingly argued that olivine-hosted melt inclusions better sample the existing spectrum of primitive/parental magma compositions produced during partial melting, prior to their homogenization in magma chambers (Sobolev and Shimizu 1993; Shimizu 1998; Lee and Stern 1998; Luhr 2001).

Implications for magma differentiation

In basaltic magmas, decreased magmatic water contents favors the fractionation of plagioclase relative to olivine and pyroxene and the generation of a tholeiitic, as opposed to a calc-alkaline, differentiation trend (Kennedy 1955; Grove and Baker 1984; Michael and Chase 1987; Sisson and Grove 1993; Gaetani et al. 1993; Danyushevsky 2001). Walker (1989) pointed out that

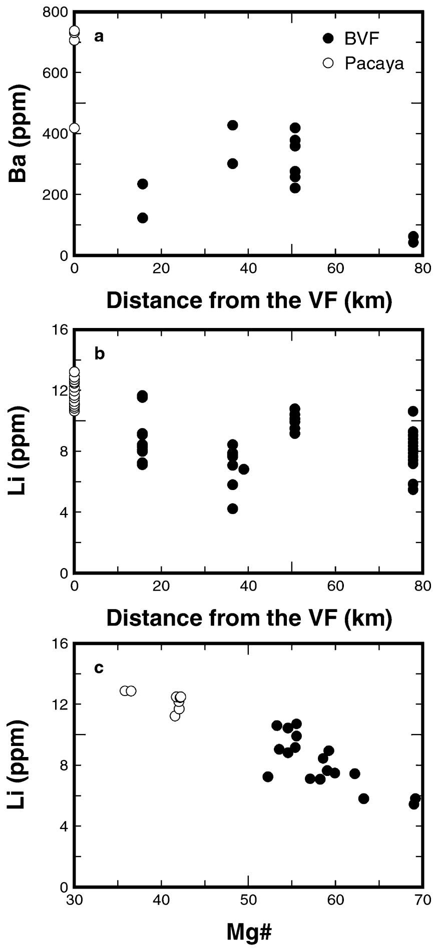

Fig. 8 Concentrations of Ba (**a**) and Li (**b**) in olivine-hosted melt inclusions across southeastern Guatemala. **c** shows Li variations against Mg#

Pacaya's basaltic lavas have elevated FeO^T, relative to most other Central American basalts, and a tholeiitic character. These characteristics were attributed to fractionation of basalts with relatively low water contents and/or at relatively low total pressures (Walker 1989). Since Pacaya's basaltic magmas do have lower average pre-eruptive water contents than those erupted at Fuego Volcano (and at Cerro Negro Volcano in Nicaragua; Fig. 2a), we suggest that fractionation at lower water contents may be the overriding cause of the Fe enrichment, and the attending Al depletion, at Pacaya. Comparison with available experimental data on basalt evolution at variable water contents supports this suggestion (Fig. 6). As mentioned earlier, the melt inclusions from Pacaya have even higher FeO^T than their host lavas. This discrepancy between melt inclusion and bulk rock compositions, and the related discrepancies in CaO and Al_2O_3, we attribute to moderate plagioclase accumulation in the host lavas (Figs. 6, 10).

Although they rarely contain clinopyroxene phenocrysts, BVF lavas bear compositional evidence of substantial clinopyroxene fractionation, such as declining CaO/Al_2O_3 with decreasing MgO (Fig. 10). To resolve this contradiction, Walker(1981) suggested that BVF magmas experienced cotectic crystallization of clinopyroxene, olivine and plagioclase at moderate pressures (0.5–1 GPa) in the lower crust, followed by rapid ascent in an extensional environment. The BVF melt inclusions also grossly exhibit declining CaO/Al_2O_3 with decreasing MgO (Fig. 10) similarly suggesting clinopyroxene control during fractionation. Judging from compositional variations defined by olivine-hosted melt inclusions from other subduction zone suites, early fractionation of significant clinopyroxene may be a common element of arc basalt genesis (Gaetani et al. 1993; Gioncada et al. 1998; Métrich et al. 1999). This is supported by recent experimental evidence which shows that arc basalt fractionation at Moho pressures with moderate-high water contents should indeed produce abundant pyroxenites (Müntener et al. 2001).

Implications for magma generation

Existing framework

Basaltic lavas erupted behind the volcanic front in southeastern Guatemala have many compositional distinctions from those erupted at the volcanic front (Walker 1981; Walker et al. 1995, 2000). Moreover, most of these distinctions appear immediately behind the front and remain relatively constant with increasing distances behind the front, as exemplified by Ba/La ratios (Fig. 9d). Hence, whole-rock basalt compositions display none of the progressive geochemical variations that commonly occur across other subduction zones (Gill 1981; Woodhead and Johnson 1993; Ishikawa and Nakamura 1994; Ryan et al. 1995, 1996; Noll et al. 1996; Hoogewerff et al. 1997; Shibata and Nakamura 1997; Ishikawa and Tera 1997; Patino et al. 1997; Barragan et al. 1998; Woodhead et al. 1998; Moriguti and Nakamura 1998; Churikova et al. 2001).

Walker et al. (1995) proposed that the abrupt across-arc discontinuities in tracers of fluid influence from the subducted slab, such as the Ba/La ratio, were an indication that slab input declines abruptly behind the volcanic front and, as a consequence, that BVF melt generation is governed largely by decompression, rather than by the hydrous flux from the subducted plate. However, behind-the-front basalts are not totally devoid of a slab signature, as shown, for example, by their elevated ratios of Ba/La and of other fluid mobile (FM) to relatively fluid immobile elements (FI), relative to oceanic basalts (Fig. 9; Walker et al. 2000). The elevated FM/FI ratios can perhaps be reconciled with decompression melting if the slab signature stems from an earlier enrichment of the mantle wedge that preceded recent melt generation. Decoupling of specific episodes of slab dehydration and magma generation has been suggested elsewhere in Central America and in the New Britain and Bismarck island arcs (Gill et al. 1993; Reagan et al. 1994; Clark et al. 1998; Woodhead et al.

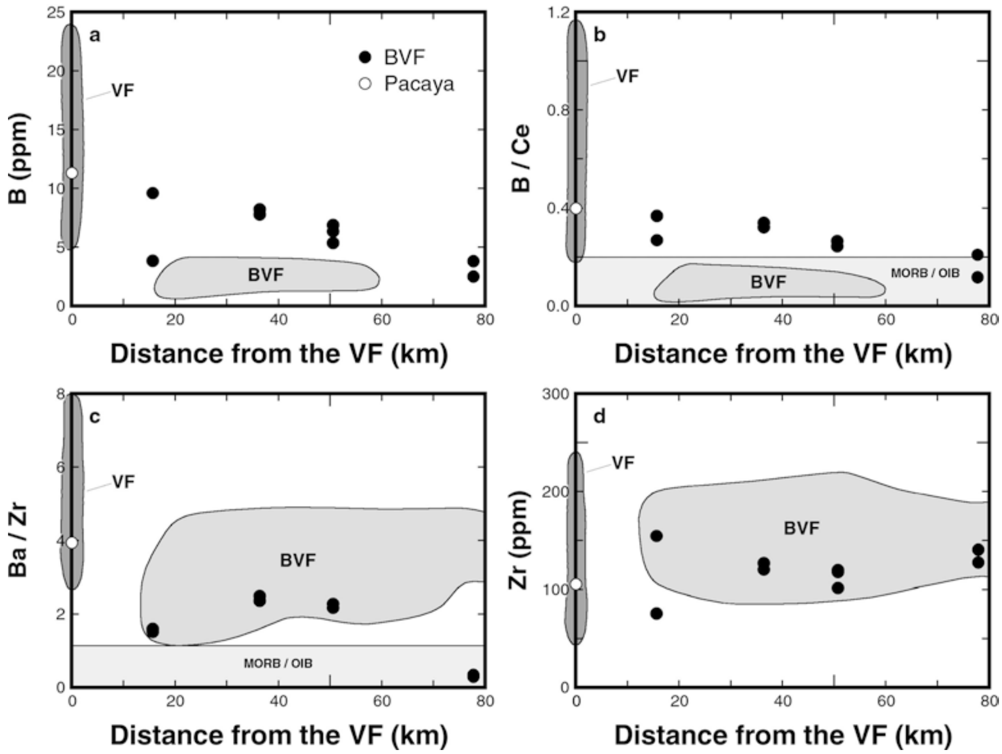

Fig. 9 Variations of B (**a**), B/Ce (**b**), Ba/Zr (**c**) and Zr (**d**) in olivine-hosted melt inclusions (*circles*), and unaltered VF and BVF lavas (*labeled fields*), across southeastern Guatemala. *Shaded* MORB/OIB band encloses inferred mantle sources of mid-ocean ridge and ocean-island basalts (Sun and McDonough 1989; Ryan and Langmuir 1993)

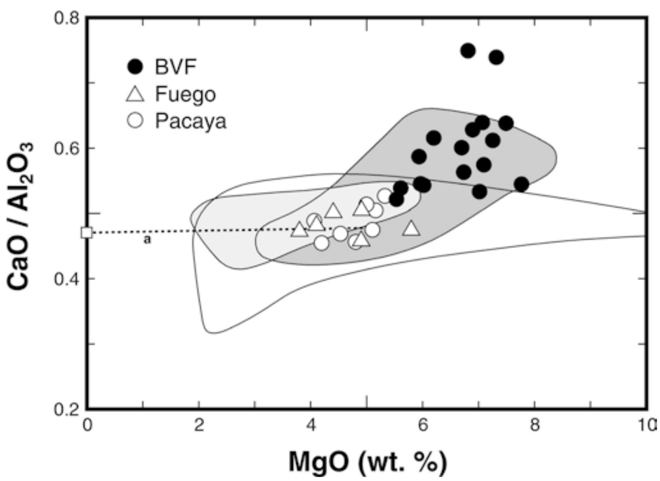

Fig. 10 CaO/Al_2O_3 versus MgO for melt inclusions from southeastern Guatemala. Where necessary, compositions have been recalculated for post-entrapment crystallization. *Fields*, *line a* and *box* as in Fig. 6

1998). Walker et al. (2000) also presented geochemical evidence that melt generation behind the front results in lower overall degrees of melting and involves a source with increasing relative contributions from subducted carbonate sediments.

Cameron et al. (2002) have recently suggested that decompression melting may also contribute significantly to magma generation beneath selected VF volcanoes of southeastern Guatemala. Specifically, both Pacaya and Agua volcanoes erupt basalts with relatively low FM/FI ratios, in some cases equivalent to those of BVF basalts (Fig. 9; Cameron et al. 2002). Magma generation beneath both is likely influenced by the active intra-arc extension experienced south of the North American/Caribbean plate boundary (Fig. 1; Burkart and Self 1985). Indeed, Pacaya lies at the southern end of the active, north-south trending Guatemala City graben where it intersects the dextral Jalpatagua fault (Fig. 1; Carr 1976).

Flux versus decompression melting

Comparisons between the measured water contents of subduction zone and mid-ocean ridge basalts (Fig. 3; Newman et al. 2000) suggest that magmatic water contents ≥1 wt% can be related to addition of a hydrous component from the subducted slab and subsequent fluid-induced (or flux-) melting (Stolper and Newman 1994). Therefore, the rare subduction zone basalts with undegassed water contents ≤ 0.5 wt% have been attributed to decompression, and not flux-, melting (Sisson and Layne 1993; Sisson and Bronto 1998). The moderate to high water contents of most basaltic magmas erupted throughout southeastern Guatemala (Figs. 2a, 3) imply that flux-melting remains an important element of magma generation across the entire region, contrary to previous suppositions (Walker et al. 1995, 2000; Cameron et al. 2002). As mentioned earlier, decompression melting is not necessarily incompatible with a strong slab signature if the latter has been stored in the mantle wedge and is not the ultimate cause of melting. However, we doubt that wedge melting beneath southeastern Guatemala is completely decoupled from recent slab dehydration for a number of reasons. First, the elevated B/Ce ratios of the melt inclusions, relative to those in MORB and OIB, suggests "recent" addition of slab fluids across southeastern Guatemala, as B is thought to have a short residence time in the mantle wedge (Hochstaedter et al. 1996). Second, the progressive across-arc declines in B/Ce, where both elements are of similar incompatibility in magmas, would seem to warrant an intrinsic link between fluid input and wedge melting (e.g., Ryan et al. 1996). Third, the negative correlations between water and some FI trace elements (Fig. 5) can be nicely rationalized by flux-melting (i.e., more slab fluids [higher water contents] yield higher degrees of melting [lower FI contents]; Stolper and Newman 1994). Decompression-derived basalts from the Juan de Fuca Ridge, by contrast, display positive correlations between H_2O and FI trace elements (Dixon et al. 1988). Fourth, lavas from selected behind-the-front volcanoes in other arcs that show progressive across-arc changes in FM/FI ratios also exhibit some $^{238}U-^{230}Th$ disequilibrium suggesting recent (≤ 350,000 years) U enrichment of the mantle wedge by slab-derived fluids and a close relationship between dehydration and magma generation (Gill et al. 1993; Hoogewerff et al. 1997).

Although the new volatile and trace element data from olivine-hosted melt inclusions suggest that partial melting remains intimately tied to slab dehydration in a slice across the Central American subduction zone, we still believe that there is a significant component of decompression-driven melting behind the volcanic front and below the VF volcanoes bordering the Guatemala City graben, i.e., Pacaya Volcano and Agua Volcano. Flux melting should produce direct correlations between measures of slab input and measures of the degree of melting (Ryan et al. 1996; Walker et al. 2000; Clift et al. 2001; Cameron et al. 2002). Fig. 11 shows that the new trace element data from BVF and Pacaya melt inclusions are consistent with existing whole-rock data which display minimal variation in slab input (B/Ce) with degree of melting (Zr/Y), a trend indicative of decompression rather than flux melting.

In sum, we propose that melt generation across southeastern Guatemala is driven by both decompression and additions of slab fluids (Pearce and Parkinson 1993). Similar conclusions have been reached for magma generation in the Mariana Trough and the Shasta-Medicine Lake area of the Cascades (Stolper and Newman 1994; Kinzler et al. 2000; Grove et al. 2002). The trace element data in Fig. 11 can be used to estimate the relative contributions from flux- versus decompression melting. The BVF composition with the lowest B/Ce ratio can be produced by about 4–5% (decompression) partial melting of anhydrous mantle peridotite (Fig. 11). These percentages of melting are compatible with previous estimates for BVF magmas using so-called wedge-controlled (or fluid immobile) elements (Walker et al. 1995). As shown in Fig. 11, the B/Ce ratios of other BVF magmas and VF magmas from Pacaya and

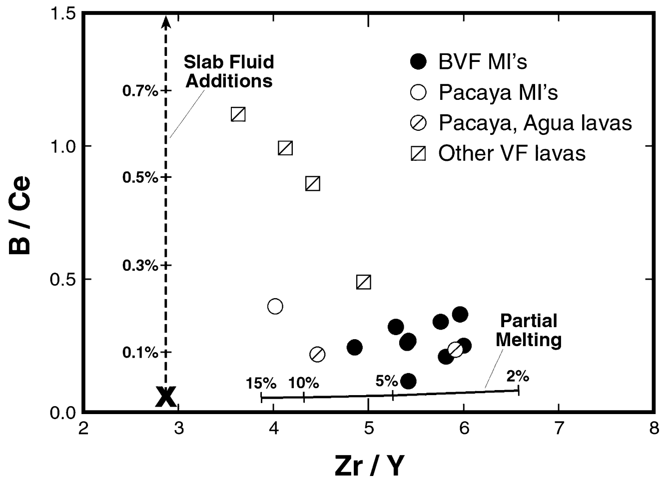

Fig. 11 B/Ce against Zr/Y for melt inclusions and VF lavas from southeastern Guatemala. *Solid line* is a partial melting model showing 2–15% batch melting of a MORB source (*large X*). Trace element concentrations of MORB source from Leeman et al. (1994), Bizimis et al. (2000), and Stolper and Newman (1994). Bulk distribution coefficient for B from Ryan and Langmuir (1993); others calculated from melting model and partition coefficients of Bizimis et al. (2000). *Dashed line* shows addition of 0.1–0.7% slab fluid to MORB source. The slab fluid is assumed to have 90, 1.6, 16 and 6 ppm of B, Ce, Zr, and Y, respectively. These values, except for Y, are taken from Leeman et al. (1994) and Bizimis et al. (2000). The Y concentration of the slab fluid was calculated such that the Zr/Y of the mantle source and slab fluid were equivalent

Agua suggest they contain approximately 0.1–0.3% of a fluid component from the subducted slab. Magmas from other Guatemalan VF volcanoes, by contrast, clearly possess larger percentages of a slab fluid component (~0.5–0.7%; Fig. 11), percentages consistent with recent estimates from other subduction zone volcanoes (Eiler et al. 2000; Bizimis et al. 2000; Churikova et al. 2001). Using the algorithm of Stolper and Newman (1994; Fig. 6), addition of 0.1–0.3% and ≥0.5% of a H_2O-rich component to the mantle wedge will produce approximately 3–8% and ≥14% partial melting, respectively. Assuming these amounts of flux-melting are superimposed on a maximum of 5% decompression melting, then the minimum relative contributions of flux to decompression melting are about 1:1 for magma generation below BVF volcanoes, Pacaya and Agua; and above 3:1 for other Guatemalan VF volcanoes.

Melting of pyroxenites?

The CaO-rich melt inclusions from Cerro Las Ruedas, the cinder cone farthest from the volcanic front, are chemically similar to distinctly CaO-rich olivine-hosted melt inclusions found in a number of terrestrial subduction zones (Metrich and Clocchiatti 1996; Della-Pasqua and Varne 1997; Sisson and Bronto 1998; Gioncada et al. 1998; Métrich et al. 1999; Schiano et al. 2000; De Hoog et al. 2001). These unusual melt inclusions and correspondent CaO-rich whole-rock compositions from subduction zones have been comprehensively studied by Della-Paqua and Varne (1997) and Schiano et al. (2000). Both conclude that such CaO-rich melts are a distinctive brand of primitive magma generated in arc environments, although ultra-calcic melt inclusions have been found in a variety of tectonic environments (e.g., Kogiso and Hirschmann 2001). Della-Pasqua and Varne (1997) suggested that CaO-rich arc magmas may be produced by partial melting of peridotite at high pressures (4–5 GPa) or of carbonated peridotite in the mantle wedge. In contrast, Schiano et al. (2000) cogently argue that such compositions are generated at subduction zones by the partial melting of CaO-rich pyroxenites in the uppermost mantle wedge or lowermost crust (see also Barsdell and Berry 1990; Kamenetsky and Clocchiatti 1996; Sisson and Bronto 1998; De Hoog et al. 2001). Although a detailed discussion of the origin of CaO-rich arc magmas is beyond the scope of this paper, we note that the two CaO-rich BVF melt inclusions have the highest concentrations of CO_2 (≥2,000 ppm; Fig. 12) suggesting they originated from a CO_2-rich source. A CO_2-rich source would be consistent with the proposal of Walker et al. (2000) for enhanced contributions of subducting carbonate sediments to the slab flux in the BVF region. Existing theoretical modeling, however, indicates minimal devolatilization of subducted carbonate sediments between 80 and 180 km depths unless induced by the infiltration of H_2O-rich fluids (Kerrick and Connolly 2001).

Suggested geodynamic model for magma generation

Above we concluded that hydrous fluids from the subducting Cocos plate remain important catalysts for magma generation across southeastern Guatemala. There is growing petrological and geophysical evidence that hydrous phases can persist in the slab/wedge region to depths exceeding 300 km, depending on the thermal structure of the subduction zone (Ulmer and Trommsdorff 1995; Iwamori 1998; Schmidt and Poli 1998; Mysen et al. 1998; Abers 2000; Ulmer 2001; Wyss et al. 2001). Currently, there are two competing models for dehydration of the slab/wedge region: (1) dehydration occurs continuously or nearly continuously with depth (Schmidt and Poli 1998; Mysen et al. 1998; Ulmer 2001); (2) dehydration is ultimately tied to the breakdown of one to two critical phases at specific depths within the down-dragged portions of the mantle wedge (Tatsumi 1986; Iwamori 1998). The progressive declines in B contents and B/Ce ratios across southeastern Guatemala, and the generally systematic declines of FM/FI ratios across other subduction zones, are easier to reconcile with relatively continuous slab dehydration, during which B and other FM elements are progressively stripped from subducting lithosphere (Ryan et al. 1995; Hochstaedter et al. 2001). Moreover, Schmidt and Poli (1998) argue that the additional time required by models involving a down-dragged mantle wedge is inconsistent with the observed U-Th disequilibrium found in many arc lavas. Therefore, we assume that dehydration is relatively continuous beneath southeastern Guatemala to depths of at least 175–200 km (Fig. 13).

Once released from the slab/wedge region, hydrous fluids are often presumed to rise vertically to sub-vertically into overlying portions of the mantle wedge (McBirney 1969; Ringwood 1974; Tatsumi et al. 1983; Sakuyama and Nesbitt 1986; Tatsumi 1986; Ulmer and Trommsdorff 1985; Iwamori 1998; Schmidt and Poli 1998). Gribble et al. (1998) have even envisioned vertical movement of hydrous fluids for transfer of a slab component into the magmatic source for the Mariana Trough, much of which fails to overlie the vertically

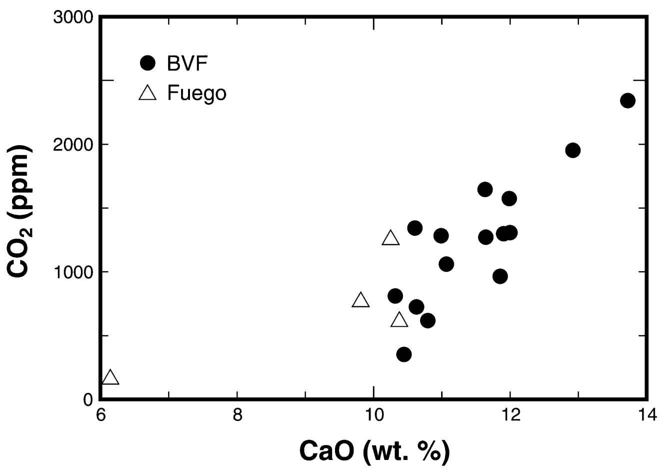

Fig. 12 CO_2 versus CaO for olivine-hosted melt inclusions from Fuego and BVF cinder cones. Where necessary, CaO was recalculated for post-entrapment crystallization (see text)

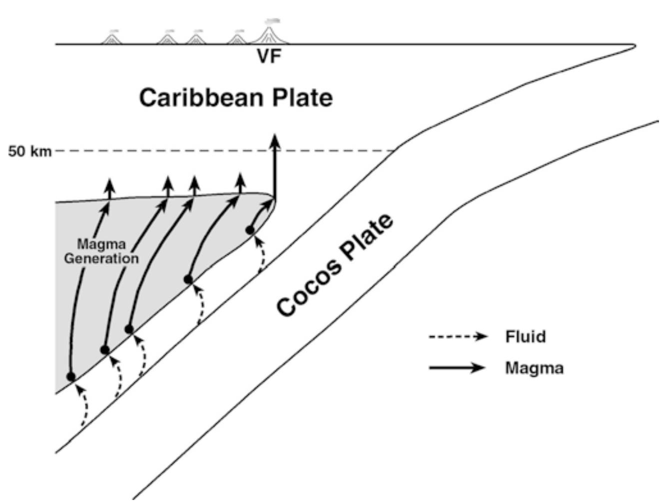

Fig. 13 Suggested configuration of magma generation across southeastern Guatemala in which deep dehydration triggers partial melting in the overlying mantle wedge. The resultant magmas become influenced by mantle counterflow, but not to the extent of "normal" subduction zones due to significant arc-normal extension (see Ribe 1989). Hence, the proliferation of back-arc or behind-the-front volcanoes

plunging Pacific plate. According to Gribble et al. (1998), vertical slab transfer occurred earlier, during intra-arc rifting and before the establishment of a sea-floor spreading regime. Nevertheless, Davies and Stevenson (1992) have proposed an alternative mechanism of slab transfer in which water migrates laterally from the subducted slab to the zone of wedge melting. Lateral migration is accomplished in zigzag fashion through a series of dehydration steps in the mantle wedge until melting occurs at the amphibole peridotite solidus. One potential problem with the Davies and Stevenson (1992) model is that the additional time required for the multiple dehydration steps may also be incompatible with the observed U-Th disequilibrium found in many arc lavas (Schmidt and Poli 1998). In addition, experimentally produced melts of amphibole peridotite are andesitic, not basaltic (Sisson et al. 1997; Schmidt and Poli 1998), i.e., not the required primary composition in Guatemala and along most subduction zones (e.g., Carr 1984; Davidson 1996). Hence, we assume that hydrous fluids rise sub-vertically into the mantle wedge once released from the subducting Cocos plate (Fig. 13).

Given this ready supply of water into the mantle wedge, magma generation becomes equally dependent on the temperature distribution in the wedge (Schmidt and Poli 1998; Ulmer 2001). Experimental constraints suggest that the production of primitive H_2O-bearing subduction zone basalts requires melting temperatures of 1,250–1,400 °C (Tatsumi et al. 1983; Tatsumi and Eggins 1995; Schmidt and Poli 1998; Sisson and Bronto 1998; Ulmer 2001). Hence, magma generation is likely focused in the hot center of the mantle wedge at depths of about 70–150 km (Fig. 13; Iwamori 1998). Magma generation in the medial portions of mantle wedges is supported by recent tomographic analyses of a number of subduction zones, which also suggest hydrous fluids often reach the zone of magma generation via equilibrium porous flow (Zhao et al. 1994, 1997; Iwamori and Zhao 2000; Tamura et al. 2002).

In many subduction zones, as first pointed out by Spiegelman and McKenzie (1987), magmas produced in the mantle wedge will be drawn upward and toward the wedge corner due to slab-induced counterflow (McKenzie 1969; Toksöz and Bird 1977). This is supported by recent tomographic studies which show that low seismic wave velocities define a zone in the mantle wedge, subparallel to the subducting plate, that extends from the back-arc region to the wedge corner (Hasegawa et al. 1991; Zhao et al. 1995, 1997, 2000; Iwamori and Zhao 2000; Wyss et al. 2001; Tamura et al. 2002). Slab-induced counterflow will thus promote the development of a narrow line of volcanoes at the surface, i.e., the volcanic front (Spiegelman and McKenzie 1987; Iwamori 1998; Schmidt and Poli 1998). Development of a narrow volcanic front may also be induced by stress transitions in and rheology of the mantle wedge (Davies and Stevenson 1992; Furukawa 1993; Billen and Gurnis 2001), or by decoupling of wedge counterflow from a buoyant, sepentinized forearc mantle (e.g., Bostock et al. 2002). However, in southeastern Guatemala, and in other subduction zones where behind-the-front or back-arc extension is significant, magma flow paths are more likely to be subvertical, rather than angled toward the wedge corner (Fig. 13; Ribe 1989). Moreover, magma generation will be less dependent on fluid fluxing from the subducting plate and more on decompression melting near the top of the wedge (Walker et al. 1995; Elkins Tanton et al. 2001). In such "extensional" subduction zones, migration of magma through the wedge could be via diapirism (Ringwood 1974; Tatsumi et al. 1983; Kushiro 1969; Hall and Kincaid 2001); porous flow (Spiegelman and McKenzie 1987; Ribe 1989; Grove et al. 2002); or fracture propagation (Davies and Stevenson 1992; Furukawa 1993).

Conclusions

Olivine-hosted melt inclusions indicate that water contents of basaltic magmas show no consistent variation, and remain moderately high ($\approx$2 wt%), over 75 km across the northern portion of the Central American arc in southeastern Guatemala. This is consistent with trace element evidence, from both melt inclusions and whole rocks, for a slab component in the back-arc, or behind-the-front, magmas of this region. Water contents remain moderately high in primitive basaltic magmas across southeastern Guatemala because there are a number of dehydration reactions that continually supply water to the overlying mantle wedge. Melting across the entire arc, therefore, is a combination of both flux-melting and decompression melting. However, decompression melting, likely focused in the upper portions of the mantle wedge, has much greater importance behind the front and at the volcanic front volcanoes associated with the Guatemala City graben. Decompression melting is enhanced in these areas because of recent back-arc and intra-arc extension. The notably high CO_2 contents in back-arc basalts may be further evidence of carbonate contributions to their magmatic source. The moderate water concentrations of the back-arc basalts has promoted the early fractionation of clinopyroxene at depth, a differentiation step that is likely common for many subduction zone basaltic magmas.

Acknowledgments Thanks are extended to J. Clark for assistance on the ASU electron microprobe (obtained with aid from NSF EAR-8408163); J. Lowenstern (USGS, Menlo Park) for access to his FTIR laboratory; R. Hervig for assistance with the ion probe analyses; M. Howland for expertly drafting the figures; C. Augustine and INSIVUMEH for help in the field; and T. Sisson and G. Müntener for suggesting significant improvements to the manuscript. This work was supported by NSF grant EAR-9873575.

References

Abers GA (2000) Hydrated subducted crust at 100–250 km depth. Earth Planet Sci Lett 176:323–330

Aggrey KE, Muenow DW, Batiza R (1988a) Volatile abundances in basaltic glasses from seamounts flanking the East Pacific Rise at 21°N and 12–14°N. Geochim Cosmochim Acta 52:2115–2119

Aggrey KE, Muenow DW, Sinton JM (1988b) Volatile abundances in submarine glasses from the North Fiji and Lau back-arc basins. Geochim Cosmochim Acta 52:2501–2506

Anderson AT Jr (1974) Evidence for a picritic, volatile-rich magma beneath Mt. Shasta, California. J Petrol 15:243–267

Baker DR, Eggler DH (1987) Compositions of anhydrous and hydrous melts coexisting with plagioclase, augite, and olivine or low-Ca pyroxene from 1 atm to 8 kbar: application to the Aleutian volcanic center of Atka. Am Mineral 72:12–28

Barragan R, Geist D, Hall M, Larson P, Kurz M (1998) Subduction controls on the compositions of lavas from the Ecuadorian Andes. Earth Planet Sci Lett 154:153–166

Barsdell M, Berry RF (1990) Origin and evolution of primitive island arc ankaramites from western Epi, Vanuatu. J Petrol 31:747–777

Billen MI, Gurnis M (2001) A low viscosity wedge in subduction zones. Earth Planet Sci Lett 193:227–236

Bizimis M, Salters VJM, Bonatti E (2000) Trace and REE content of clinopyroxenes from supra-subduction zone peridotites. Implications for melting and enrichment processes in island arcs. Chem Geol 165:67–85

Boettcher AL (1977) The role of amphiboles and water in Circum-Pacific volcanism. In: Manghnani MH, Akimoto S (eds) High Pressure Research. Applications in Geophysics. Academic Press, New York, pp 107–125

Bostock MG, Hyndman RD, Rondenay S, Peacock SM (2002) An inverted continental Moho and serpentinization of the forearc mantle. Nature 417:536–538

Bureau H, Pineau F, Métrich N, Semet MP, Javoy M (1998a) A melt and fluid inclusion study of the gas phase at Piton de la Fournaise Volcano (Réunion Island). Chem Geol 147:115–130

Bureau H, Métrich N, Pineau F, Semet MP (1998b) Magma-conduit interaction at Piton de la Fournaise Volcano (Réunion Island): a melt and fluid inclusion study. J Volcanol Geotherm Res 84:39–60

Burkart B, Self S (1985) Extension and rotation of crustal blocks in northern Central America and effect on the volcanic arc. Geology 13:22–26

Byers CD, Muenow DW, Garcia MO (1983) Volatiles in basalts and andesites from the Galapagos Spreading Center, 85° to 86°W. Geochim Cosmochim Acta 47:1551–1558

Byers CD, Garcia MO, Muenow DW (1985) Volatiles in pillow rim glasses from Loihi and Kilauea volcanoes, Hawaii. Geochim Cosmochim Acta 49:1887–1896

Byers CD, Garcia MO, Muenow DW (1986) Volatiles in basaltic glasses from the East Pacific Rise at 21°N: implications for MORB sources and submarine lava flow morphology. Earth Planet Sci Lett 79:9-20

Cameron BI (1998) Melt generation and magma evolution in southeastern Guatemala. PhD Thesis, Northern Illinois University, DeKalb, IL

Cameron BI, Walker JA, Carr MJ, Patino LC, Matías O, Feigenson MD (2002) Flux versus decompression melting at stratovolcanoes in southeastern Guatemala. J Volcanol Geotherm Res (in press)

Carr MJ (1976) Underthrusting and Quaternary faulting in northern Central America. Geol Soc Am Bull 87:825–829

Carr MJ (1984) Symmetrical and segmented variation of physical and geochemical characteristics of the Central American volcanic front. J Volcanol Geotherm Res 20:231–252

Carr MJ, Mayfield DG, Walker JA (1981) Relation of lava compositions to volcano size and structure. J Volcanol Geotherm Res 10:35–48

Cawthorn RG, O'Hara MJ (1976) Amphibole fractionation in calc-alkaline magma genesis. Am J Sci 276:309–329

Cervantes P, Wallace P (2003) Magma degassing and basaltic eruption styles: a case study of ~2000 year BP Xitle Volcano in central Mexico: J Volcanol Geotherm Res 120:249–270

Churikova T, Dorendorf F, Wörner G (2001) Sources and fluids in the mantle wedge below Kamcahtka, evidence from across-arc geochemical variation. J Petrol 42:1567–1593

Clark SK, Reagan MK, Plank T (1998) Trace element and U-series systematics for 1963–1965 tephras from Irazú Volcano, Costa Rica: implications for magma generation processes and transit times. Geochim Cosmochim Acta 62:2689–2699

Clift PD, Rose EF, Shimizu N, Layne GD, Draut AE, Regelous M (2001) Tracing the evolving flux from the subducting plate in the Tonga-Kermadec arc system using boron in volcanic glass. Geochim Cosmochim Acta 65:3347–3364

Clocchiatti R (1975) Les inclusions vitreuses des cristaux de quartz. Etude optique, thermo-optique et chimique. Applications géologiques. Mém Soc Géol Fr 54:1–96

Danyushevsky LV (2001) The effect of small amounts of H_2O on crystallization of mid-ocean ridge and backarc magmas. J Volcanol Geotherm Res 110:265–280

Danyushevsky LV, Falloon TJ, Sobolev AV, Crawford AJ, Carroll M, Price RC (1993) The H_2O content of basalt glasses from southwest Pacific back-arc basins. Earth Planet Sci Lett 117:347–362

Danyushevsky LV, Della-Pasqua FN, Sokolov S (2000) Re-equilibration of melt inclusions trapped by magnesian olivine phenocrysts from subduction-related magmas: petrological implications. Contrib Mineral Petrol 138:63–83

Davidson JP (1996) Deciphering mantle and crustal signatures in subduction zone magmatism. In: Bebout GE, Scholl DW, Kirby SH, Platt JP (eds) Subduction: top to bottom. Am Geophys Union Geophys Monograph 96, pp 251–262

Davies JH, Stevenson DJ (1992) Physical model of source region of subduction zone volcanics. J Geophys Res 97:2037–2070

De Hoog JCM, Mason PRD, Van Bergen MJ (2001) Sulfur and chalcophile elements in subduction zones: constraints from a laser ablation ICP-MS study of melt inclusions from Galunggung Volcano, Indonesia. Geochim Cosmochim Acta 65:3147–3164

Della-Pasqua FN, Varne R (1997) Primitive ankaramitic magmas in volcanic arcs: a melt-inclusion approach. Can Mineral 35:291–312

Dixon JE, Stolper EM (1995) An experimental study of water and carbon dioxide solubilities in mid-ocean ridge basaltic liquids. Part II: applications to degassing. J Petrol 36:1633–1646

Dixon JE, Stolper E, Delaney JR (1988) Infrared spectroscopic measurements of CO_2 and H_2O in Juan de Fuca Ridge basaltic glasses. Earth Planet Sci Lett 90:87–104

Eiler JM, Crawford A, Elliott T, Farley KA, Valley JW, Stolper EM (2000) Oxygen isotope geochemistry of oceanic-arc lavas. J Petrol 41:229–256

Elkins Tanton LT, Grove TL, Donnelly-Nolan J (2001) Hot, shallow mantle melting under the Cascades volcanic arc. Geology 29:631–634

Furukawa Y (1993) Magmatic processes under arcs and formation of the volcanic front. J Geophys Res 98:8309–8319

Gaetani GA, Grove TL (1998) The influence of water on melting of mantle peridotite. Contrib Mineral Petrol 131:323–346

Gaetani GA, Watson EB (2000) Open system behavior of olivine-hosted melt inclusions. Earth Planet Sci Lett 183:27–41

Gaetani GA, Grove TL, Bryan WB (1993) The influence of water on the petrogenesis of subduction-related igneous rocks. Nature 365:332–334

Garcia MO, Liu NWK, Muenow DW (1979) Volatiles in submarine volcanic rocks from the Mariana Island arc and trough. Geochim Cosmochim Acta 43:305–312

Gill JB (1981) Orogenic andesites and plate tectonics. Springer, Berlin Heidelberg New York

Gill JB, Morris JD, Johnson RW (1993) Timescale for producing the geochemical signature of island arc magmas: U–Th–Po and Be–B systematics in recent Papua New Guinea lavas. Geochim Cosmochim Acta 57:4629–4283

Gioncada A, Clocchiatti R, Sbrana A, Bottazzi P, Massare D, Ottolini L (1998) A study of melt inclusions at Vulcano (Aeolian Islands, Italy): insights on the primitive magmas and on the volcanic feeding system. Bull Volcanol 60:286–306

Green DH (1973) Experimental melting studies on a model upper mantle composition at high pressure under water-saturated and water-undersaturated conditions. Earth Planet Sci Lett 19:37–53

Gribble RF, Stern RJ, Newman S, Bloomer SH, O'Hearn T (1998) Chemical and isotopic composition of lavas from the Northern Mariana Trough: implications for magmagenesis in back-arc basins. J Petrol 39:125–154

Grove TL, Baker MB (1984) Phase equilibrium controls on the tholeiitic versus calc-alkaline differentiation trends. J Geophys Res 89:3253–3274

Grove TL, Parman SW, Bowring SA, Price RC, Baker MB (2002) The role of an H_2O-rich fluid component in the generation of primitive basaltic andesites and andesites from the Mt. Shasta region, N California. Contrib Mineral Petrol 142:375–396

Hall PS, Kincaid C (2001) Diapiric flow at subduction zones: a recipe for rapid transport. Science 292:2472–2475

Harris DM, Anderson AT (1984) Volatiles H_2O, CO_2, and Cl in a subduction related basalts. Contrib Mineral Petrol 87:120–128

Hasegawa A, Zhao D, Hori S, Yamamoto A, Horiuchi S (1991) Deep structure of the northeastern Japan arc and its relationship to seismic and volcanic activity. Nature 352:683–689

Higgins MD (1988) Trace element geochemistry of the Inyo volcanic chain, California: evidence for multiple magma sources, magma mixing and post-eruption loss of boron. J Volcanol Geotherm Res 35:97–110

Hirose K, Kawamoto T (1995) Hydrous partial melting of lherzolite at 1 GPa: the effect of H_2O on the genesis of basaltic magmas. Earth Planet Sci Lett 133:463–473

Hochstaedter AG, Gill JB, Kusakabe M, Newman S, Pringle M, Taylor B, Fryer P (1990) Volcanism in the Sumisu Rift, I. Major element, volatile, and stable isotope geochemistry. Earth Planet Sci Lett 100:179–194

Hochstaedter AG, Ryan JG, Luhr JF, Hasenaka T (1996) On B/Be ratios in the Mexican volcanic belt. Geochim Cosmochim Acta 60:613–628

Hochstaedter A, Gill J, Peters R, Broughton P, Holden P (2001) Across-arc geochemical trends in the Izu-Bonin arc: contributions from the subducting slab. Geochem Geophys Geosys 2:2000GC000105

Hoogewerff JA, van Bergen MJ, Vroon PZ, Hertogen J, Wordel R, Sneyers A, Nasution A, Varekamp JC, Moens, HLE, Mouchel D (1997) U-series, Sr-Nd-Pb isotope and trace-element systematics across an active island arc-continent collision zone: implications for element transfer at the slab-wedge interface. Geochim Cosmochim Acta 61:1057–1072

Ishikawa T, Nakamura E (1994) Origin of the slab component in arc lavas from across-arc variation of B and Pb isotopes. Nature 370:205–208

Ishikawa T, Tera F (1997) Source, composition and distribution of the fluid in the Kurile mantle wedge: constraints from across-arc variations of B/Nb and B isotopes. Earth Planet Sci Lett 152:123–138

Iwamori H (1998) Transportation of H_2O and melting in subduction zones. Earth Planet Sci Lett 160:65–80

Iwamori H, Zhao D (2000) Melting and seismic structure beneath the northeast Japan arc. Geophys Res Lett 27:425–428

Jambon A, Zimmerman JL (1988) Water in oceanic basalts: evidence for dehydration of recycled crust. Earth Planet Sci Lett 101:323–331

Kamenetsky V, Clocchiatti R (1996) Primitive magmatism of Mt. Etna: insights from mineralogy and melt inclusions. Earth Planet Sci Lett 142:553–572

Kamenetsky V, Métrich N, Cioni R (1995) Potassic primary melts of Vulsini (Roman Province): evidence from mineralogy and melt inclusions. Contrib Mineral Petrol 120:186–196

Kennedy GC (1955) Some aspects of the role of water in rock melts. In: Poldervaart A (ed) Crust of the Earth (a symposium). Geol Soc Am Spec Pap 62:489–503

Kerrick DM, Connolly JAD (2001) Metamorphic devolatilization of subducted marine sediments and the transport of volatiles into the Earth's mantle. Nature 411:293–296

Kinzler RJ, Donnelly-Nolan JM, Grove TL (2000) Late Holocene hydrous mafic magmatism at the Paint Pot crater and Callahan flows, Medicine Lake Volcano, N. California and the influence of H_2O in the generation of silicic magmas. Contrib Mineral Petrol 138:1–16

Kogiso T, Hirschmann MM (2001) Experimental study of clinopyroxenite partial melting and the origin of ultra-calcic melt inclusions. Contrib Mineral Petrol 142:347–360

Kushiro I (1969) The system forsterite-diopside-silica with and without water at high pressures. Am J Sci 267-A:269–294

Kushiro I (1972) Effect of water on the compositions of magmas formed at high pressures. J Petrol 13:311–334

Lee J, Stern RJ (1998) Glass inclusions in Mariana arc phenocrysts: a new perspective on magmatic evolution in a typical intra-oceanic arc. J Geol 106:19–33

Leeman WP, Carr MJ, Morris JD (1994) Boron geochemistry of the Central American volcanic arc: constraints on the genesis of subduction-related magmas. Geochim Cosmochim Acta 58:149–168

Luhr JF (2001) Glass inclusions and melt volatile contents at Parícutin Volcano, Mexico. Contrib Mineral Petrol 142:261–283

Marianelli P, Métrich N, Sbrana A (1999) Shallow and deep reservoirs involved in magma supply of the 1944 eruption of Vesuvius. Bull Volcanol 61:48–63

McBirney AR (1969) Compositional variations in Cenozoic calc-alkaline suites of Central America. In: McBirney AR (ed) Proceedings of the Andesite Conference. Oregon Dept Geol Mineral Res, Bull 65, pp 185–189

McKenzie DP (1969) Speculations on the consequences and causes of plate motions. Geophys J Roy Soc Lond 18:1–32

Metrich N, Clocchiatti R (1996) Sulfur abundance and its speciation in oxidized alkaline melts. Geochim Cosmochim Acta 60:4151–4160

Métrich N, Schiano P, Clocchiatti R, Maury RC (1999) Transfer of sulfur in subduction settings: an example from Batan Island (Luzon volcanic arc, Philippines). Earth Planet Sci Lett 167: 1–14

Michael P (1988) The concentration, behavior and storage of H_2O in the suboceanic upper mantle: implications for mantle metasomatism. Geochim Cosmochim Acta 52:555–566

Michael PJ, Chase RL (1987) The influence of primary magma composition, H_2O and pressure on Mid-Ocean Ridge basalt differentiation. Contrib Mineral Petrol 96:245–263

Moriguti T, Nakamura E (1998) Across-arc variation of Li isotopes in lavas and implications for crust/mantle recycling at subduction zones. Earth Planet Sci Lett 163:167–174

Morrice MG, Gill JB (1986) Spatial patterns in the mineralogy of island arc magma series: Sangihe arc, Indonesia. J Volcanol Geotherm Res 29:311–353

Muenow DW, Garcia MO, Aggrey KE, Bednarz U, Schmincke HU (1990) Volatiles in submarine glasses as a discriminant of tectonic origin: application to the Troodos ophiolite. Nature 343:159–161

Müntener O, Kelemen PB, Grove TL (2001) The role of H_2O during crystallization of primitive arc magmas under uppermost mantle conditions and genesis of igneous pyroxenites: an experimental study. Contrib Mineral Petrol 141:643–658

Mysen BO, Boettcher AL (1975) Melting of hydrous mantle: II. Geochemistry of crystals and liquids formed by anatexis of mantle peridotite at high pressures and high temperatures as a function of controlled activities of water, hydrogen, and carbon dioxide. J Petrol 16:549–593

Mysen BO, Ulmer P, Konzett J, Schmidt MW (1998) The upper mantle near convergent plate boundaries. In: Hemley RJ (ed) Ultrahigh-pressure mineralogy; Physics and chemistry of the Earth's deep interior. Rev Mineral 37:97–138

Newman S, Lowenstern JB (2002) VolatileCalc; a silicate melt-H_2O-CO_2 solution model written in Visual Basic for Excel. Comput Geosci 28:597–604

Newman S, Stolper E, Stern R (2000) H_2O and CO_2 in magmas from the Mariana arc and back arc systems. Geochem Geophys Geosyst 1:1999GC000027
Noll PD Jr, Newsom HE, Leeman WP, Ryan JG (1996) The role of hydrothermal fluids in the production of subduction zone magmas: evidence from siderophile and chalcophile trace elements and boron. Geochim Cosmochim Acta 60:587–611
Norman MD, Pearson NJ, Sharma A, Griffin WL (1996) Quantitative analyses of trace elements in geological materials by laser ablation ICPMS: instrumental operating conditions and calibration values of NIST glasses. Geostand News 20:247–261
Osborn EF (1959) Role of oxygen pressure in the crystallization and differentiation of basaltic magma. Am J Sci 257:609–647
Patino LC, Carr MJ, Feigenson MD (1997) Cross-arc geochemical variations in volcanic fields in Honduras C.A.: progressive changes in source with distance from the volcanic front. Contrib Mineral Petrol 129:341–351
Patino LC, Samuels AC, Carr MJ, Feigenson MD (1998) The effects of weathering on the REE profiles of lavas from southeast Guatemala. Geol Soc Am Abstr Progr 30:92
Patino LC, Carr MJ, Feigenson MD (2000) Local and regional variations in Central American arc lavas controlled by variations in subducted sediment input. Contrib Mineral Petrol 138:265–283
Patino LC, Wade J, Anderson A, Velbel M (2002) Effects of incipient weathering in the composition of basalts and andesites from Guatemala. Geol Soc Am Abstr Progr 34:A-122
Pearce JA, Parkinson IJ (1993) Trace element models for mantle melting: application to volcanic arc petrogenesis. In: Prichard HM, Alabaster T, Harris NBW, Neary CR (eds) Magmatic processes and plate tectonics. Geol Soc Spec Publ 76:373–403
Reagan MK, Morris, JD, Herrstrom EA, Murrell MT (1994) Uranium series and beryllium isotope evidence for an extended history of subduction modification of the mantle below Nicaragua. Geochim Cosmochim Acta 58:4199–4212
Ribe NM (1989) Mantle flow induced by back arc spreading. Geophys J Int 98:85–91
Ringwood AE (1974) The petrological evolution of island arc systems. J Geol Soc Lond 130:183–204
Roedder E (1984) Fluid inclusions. Rev Mineral 12:1–646
Roggensack K (2001a) Sizing up crystals and their melt inclusions: a new approach to crystallization studies. Earth Planet Sci Lett 187:221–237
Roggensack K (2001b) Unraveling the 1974 eruption of Fuego volcano (Guatemala) with small crystals and their young melt inclusions. Geology 29:911–914
Roggensack K, Williams SN, Schaefer SJ, Parnell RA (1996) Volatiles from the 1994 eruptions of Rabaul: understanding large caldera systems. Science 273:490–493
Roggensack K, Hervig RL, McKnight SB, Williams SN (1997) Explosive basaltic volcanism from Cerro Negro Volcano: influence of volatiles on eruptive style. Science 277:1639–1642
Ryan JG, Langmuir CH (1993) The systematics of boron abundances in young volcanic rocks. Geochim Cosmochim Acta 57:1489–1498
Ryan JG, Morris J, Tera F, Leeman WP, Tsvetkov A (1995) Cross-arc geochemical variations in the Kurile arc as a function of slab depth. Science 270:625–627
Ryan J, Morris J, Bebout G, Leeman B (1996) Describing chemical fluxes in subduction zones: insights from "depth-profiling" studies of arc and forearc rocks. In: Bebout GE, Scholl DW, Kirby SH, Platt JP (eds) Subduction top to bottom. Am Geophys Union Monograph 96, pp 263–268
Saito G, Kazahaya K, Shinohara H, Stimac J, Kawanabe Y (2001) Variation of volatile concentration in a magma system of Satsuma-Iwojima volcano deduced from melt inclusion analyses. J Volcanol Geotherm Res 108:11–31
Sakuyama M (1979) Lateral variations of H_2O contents in Quaternary magmas of northeastern Japan. Earth Planet Sci Lett 43:103–111
Sakuyama M, Nesbitt RW (1986) Geochemistry of the Quaternary volcanic rocks of the northeast Japan arc. J Volcanol Geotherm Res 29:413–450
Schiano P, Eiler JM, Hutcheon ID, Stolper EM (2000) Primitive CaO-rich, silica-undersaturated melts in island arcs: evidence for the involvement of clinopyroxene-rich lithologies in the petrogenesis of arc magmas. Geochem Geophys Geosys 1:1999GC000032
Schmidt MW, Poli S (1998) Experimentally based water budgets for dehydrating slabs and consequences for arc magma generation. Earth Planet Sci Lett 163:361–379
Schmitt AK, Kasemann S, Meixner A, Rhede D (2002) Boron in central Andean ignimbrites: implications for crustal boron cycles in an active continental margin. Chem Geol 183: 333–347
Shibata T, Nakamura E (1997) Across-arc variations of isotope and trace element compositions from Quaternary basaltic volcanic rocks in northern Japan: implications for interaction between subducted oceanic slab and mantle wedge. J Geophys Res 102:8051–8064
Shimizu N (1998) The geochemistry of olivine-hosted melt inclusions in a FAMOUS basalt ALV519–4-1. Phys Earth Planet Int 107:183–201
Sigurdsson H (2000) Volcanic episodes and rates of volcanism. In: Encyclopedia of volcanoes. Academic Press, New York, pp 271–279
Sisson TW, Bronto S (1998) Evidence for pressure-release melting beneath magmatic arcs from basalt at Galunggung, Indonesia. Nature 391:883–886
Sisson TW, Grove TL (1993) Experimental investigations of the role of H_2O in calc-alkaline differentiation and subduction zone magmatism. Contrib Mineral Petrol 113:143–166
Sisson TW, Layne GD (1993) H_2O in basalt and basaltic andesite glass inclusions from four subduction-related volcanoes. Earth Planet Sci Lett 117:619–635
Sisson TW, Hankins WB, Presnall DC (1997) Melting of amphibole lherzolite investigated in the system CMASN-H_2O. EOS Trans Am Geophys Union 78:835
Sobolev AV, Chaussidon M (1996) H_2O concentrations in primary melts from supra-subduction zones and mid-ocean ridges: implications for H_2O storage and recycling in the mantle. Earth Planet Sci Lett 137:45–55
Sobolev AV, Shimizu N (1993) Ultra-depleted primary melt included in an olivine from the Mid-Atlantic ridge. Nature 363:151–154
Spiegelman M, McKenzie D (1987) Simple 2-D models for melt extraction at mid-ocean ridges and island arcs. Earth Planet Sci Lett 83:137–152
Spulber SD, Rutherford MJ (1983) The origin of rhyolite and plagiogranite in oceanic crust: an experimental study. J Petrol 24:1-25
Stolper E, Newman S (1994) The role of water in the petrogenesis of Mariana trough magmas. Earth Planet Sci Lett 121:293–325
Sun SS, McDonough WF (1989) Chemical and isotopic systematics of oceanic basalts: implications for mantle composition and processes. In: Saunders AD, Norry MJ (eds) Magmatism in the ocean basins. Geol Soc Spec Publ 42, pp 313–345
Tamura Y, Tatsumi Y, Zhao D, Kido Y, Shukuno H (2002) Hot fingers in the mantle wedge: new insights into magma genesis in subduction zones. Earth Planet Sci Lett 197:105–116
Tatsumi Y (1986) Formation of the volcanic front in subduction zones. Geophys Res Lett 13:717–720
Tatsumi Y, Eggins S (1995) Subduction zone magmatism. Blackwell Science, Cambridge, MA
Tatsumi Y, Sakuyama M, Fukuyama H, Kushiro I (1983) Generation of arc basalt magmas and thermal structure of the mantle wedge in subduction zones. J Geophys Res 88:5815–5825
Tatsumi Y, Murasaki M, Arsadi EM, Nohda S (1991) Geochemistry of Quaternary lavas from NE Sulawesi: transfer of subduction components into the mantle wedge. Contrib Mineral Petrol 107:137–149

Toksöz MN, Bird P (1977) Formation and evolution of marginal basins and continental plateaus. In: Talwani M, Pitman WC (eds) Island arcs, deep sea trenches and back-arc basins. Am Geophys Union Maurice Ewing Series 1, pp 379–393

Ulmer P (1989) The dependence of Fe^{2+}–Mg cation-partitioning between olivine and basaltic liquid on pressure, temperature, and composition: an experimental study to 30 kbars. Contrib Mineral Petrol 101:261–273

Ulmer P (2001) Partial melting in the mantle wedge—the role of H_2O in the genesis of mantle-derived 'arc-related' magmas. Phys Earth Planet Inter 127:215–232

Ulmer P, Trommsdorff V (1995) Serpentine stability to mantle depths and subduction-related magmatism. Science 268:858–861

Walker JA (1981) Petrogenesis of lavas from cinder cone fields behind the volcanic front of Central America. J Geol 89:721–739

Walker JA (1989) Caribbean arc tholeiites. J Geophys Res 94:10,539–10,548

Walker JA, Carr MJ, Patino LC, Johnson CM, Feigenson MD, Ward RL (1995) Abrupt change in magma generation processes across the Central America arc in southeastern Guatemala: flux-dominated melting near the base of the wedge to decompression melting near the top of the wedge. Contrib Mineral Petrol 120:378–390

Walker JA, Patino LC, Cameron BI, Carr MJ (2000) Petrogenetic insights provided by compositional transects across the Central American arc: southeastern Guatemala and Honduras. J Geophys Res 105:18949–18963

Woodhead JD, Johnson RW (1993) Isotopic and trace-element profiles across the New Britain island arc, Papua New Guinea. Contrib Mineral Petrol 113:479–491

Woodhead JD, Eggins SM, Johnson RW (1998) Magma genesis in the New Britain island arc: further insights into melting and mass transfer processes. J Petrol 39:1641–1668

Wyss M, Hasegawa A, Nakajima J (2001) Source and path of magma for volcanoes in the subduction zone of northeastern Japan. Geophys Res Lett 28:1819–1822

Yoder HS Jr (1969) Calcalkalic andesites: experimental data bearing on the origin of their assumed characteristics. In: McBirney AR (ed) Proceedings of the andesite conference. Oregon Dept Geol Mineral Res, Bull 65, pp 77–89

Zhao D, Hasegawa A, Kanamori H (1994) Deep structure of Japan subduction zone as derived from local, regional, and teleseismic events. J Geophys Res 99:22313–22329

Zhao D, Christensen D, Pulpan H (1995) Tomographic imaging of the Alaska subduction zone. J Geophys Res 100:6487–6504

Zhao D, Xu Y, Wiens DA, Dorman L, Hildebrand J, Webb S (1997) Depth extent of the Lau back-arc spreading center and its relation to subduction processes. Science 278:254–257

Zhao D, Asamori K, Iwamori H (2000) Seismic structure and magmatism of the young Kyushu subduction zone. Geophys Res Lett 27:2057–2060